0026-895X/04/6606-1431–1439$20.00
MOLECULAR PHARMACOLOGY
Vol. 66, No. 6
3277/1184496
Mol Pharmacol 66:1431–1439, 2004
Printed in U.S.A.

Viral Macrophage Inflammatory Protein-II and Fractalkine (CX3CL1) Chimeras Identify Molecular Determinants of Affinity, Efficacy, and Selectivity at CX3CR1

Christopher N. Davis, Violetta Zujovic, and Jeffrey K. Harrison

Department of Pharmacology and Therapeutics, College of Medicine, University of Florida, Gainesville, Florida

Received May 27, 2004; accepted September 2, 2004

ABSTRACT

Fractalkine (FKN/CX3CL1) is a cell surface-expressed chemokine involved in many aspects of leukocyte trafficking and activation. The various structural domains of FKN play distinct roles in its ability to bind and activate its receptor, CX3CR1. A human herpesvirus 8-encoded chemokine, termed viral macrophage inflammatory protein (vMIP)-II, is structurally similar to FKN; vMIP-II is a nonselective chemokine receptor antagonist (binding multiple chemokine receptors, including CX3CR1). The goal of this study was to identify FKN determinants of selectivity for its receptor and to further refine domains important in affinity and efficacy at CX3CR1. Chimeric and insertional mutagenesis was used to generate mutants of both vMIP-II and FKN, and the expressed proteins were evaluated for chemokine receptor binding affinities and efficacy at CX3CR1. Modification of the intervening amino acids between the first two conserved cysteine residues of FKN or vMIP-II indicated a role of the X3 bulge of FKN in affinity and selectivity for CX3CR1. Substitution of the vMIP-II N terminus with that of FKN created an agonist that was just as potent and efficacious as FKN for binding and stimulating CX3CR1, whereas replacement of the FKN N terminus with the cognate domain of vMIP-II disrupted the ability of FKN to bind CX3CR1. Furthermore, the entire N terminus of FKN was necessary for the high-affinity and full agonist properties of FKN at CX3CR1. These results refine the pharmacophore for chemokine binding to and activation of CX3CR1 and demonstrate the usefulness of modified virally encoded chemokines as templates for the development of selective chemokine receptor antagonists.

Chemokines constitute a family of structurally and functionally related small proteins that are key regulators of the accumulation and activation of leukocytes into inflamed tissues. As a result, chemokines and their receptors represent a growing list of relevant therapeutic targets. These small peptides are made by a variety of cells in both the periphery and central nervous system including, but not limited to monocytes, T cells, B cells, dendritic cells, fibroblasts, endothelial cells, neutrophils, as well as neurons and glial cells (Murphy et al., 2000). Most chemokines, with the exception of the CX3C ligand, fractalkine (FKN/CX3CL1), and the CXC ligand CXCL16 (Matloubian et al., 2000) exist as secreted peptides. FKN is structurally unique in that it contains a CX3C chemokine domain attached to a mucin-like stalk, transmembrane domain, and a short intracellular region, and it exists in both membrane-bound and shed/secreted forms (Bazan et al., 1997; Pan et al., 1997). Many chemokines show considerable overlap in their receptor binding, although several bind with relative specificity. FKN is the only known ligand for CX3CR1, and it binds its receptor CX3CR1 with high affinity and specificity (Imai et al., 1997; Harrison et al., 1998).

It has been recently observed that some viruses have evolved molecular mechanisms that mimic chemokine machinery to interfere with normal host defense. One such mechanism has been identified in a viral protein encoded by Kaposi's sarcoma-associated herpesvirus/*Human herpesvirus 8*. Kaposi's sarcoma-associated herpesvirus encodes more than 15 human gene homologs, including three chemokines, which are termed viral macrophage inflammatory protein (vMIP) -I, -II, and -III (Moore et al., 1996; Nicholas et al.,

This work was supported by Institute for the Study of Aging and Public Health Service (NS34901) grants (to J.K.H.) and predoctoral fellowship awards (to C.N.D.) from the American Heart Association, Florida Affiliate Predoctoral Fellowship, and PhRMA Foundation predoctoral fellowship in pharmacology/toxicology.

Article, publication date, and citation information can be found at http://molpharm.aspetjournals.org.

doi:10.1124/mol.104.003277.

ABBREVIATIONS: FKN, fractalkine; vMIP-II, viral macrophage inflammatory protein-II; FKN-CD, fractalkine-chemokine domain; HEK, human embryonic kidney; NTA, nitrilotriacetic acid; DMEM, Dulbecco's modified Eagle's medium; RT, room temperature; FBS, fetal bovine serum; PAGE, polyacrylamide gel electrophoresis; CHO, Chinese hamster ovary; MCP-1, monocyte chemotactic protein-1; MIP-1α, macrophage inflammatory protein-1α; SDF-1α, stromal cell derived factor-1α; CCR, chemokine receptor for CC chemokines; CXCR, chemokine receptor for CXC chemokines; CX3CR, chemokine receptor for CX3C chemokines; Ni-NTA, nickel nitrilotriacetic acid.

1997). Of these three, only vMIP-II has been shown to be a chemokine receptor antagonist, binding CCR1, CCR2, CCR4, CCR5, CCR8, CCR10, CXCR3, CXCR4, XCR1, and CX3CR1 (Kledal et al., 1997; Chen et al., 1998; Luttichau et al., 2000, 2001). In a recent report, Nakano et al. (2003) demonstrated that mammalian cell-expressed vMIP-II has CCR5 agonist activity, suggesting that vMIP-II may play a role in chemotaxis of CCR5-expressing monocytes in vivo. vMIP-II has been used in a number of in vivo models and is a potent inhibitor of inflammation. Chen et al. (1998) showed that vMIP-II has anti-inflammatory activity in a rat model of experimental glomerulonephritis. The use of vMIP-II in a spinal cord injury model was shown to attenuate inflammation and cellular degeneration (Ghirnikar et al., 2000, 2001). Because vMIP-II nonselectively binds several chemokine receptors, the specific chemokine systems that were modulated by this viral protein cannot be known with certainty.

Although most chemokines bind one or more receptors within their specific subfamily, vMIP-II is the only chemokine known to bind receptors from multiple subfamilies. These unique receptor binding properties of vMIP-II make it a useful tool in studying chemokine/receptor interactions. vMIP-II is structurally very similar to FKN, suggesting that key residues in their sequences determine the respective binding properties of these peptides to CX3CR1. By using vMIP-II as a template, chimeric and insertional mutagenesis was used to alter the viral chemokine. Herein, we describe the creation and characterization of vMIP-II and FKN chimeras that display varying levels of affinity and efficacy for CX3CR1 and reduced affinity for representative CC and CXC chemokine receptors. The amino acids that lie between the first two conserved cysteine residues of FKN were modified, or inserted into vMIP-II, to determine the role of the X3 bulge in the high-affinity and selective interaction between FKN and CX3CR1. Multiple studies point to the importance of the vMIP-II N terminus in binding to CXCR4 and CCR5 (Luo et al., 2000; Zhou et al., 2000; Crump et al., 2001). In the present study, we also report the role of the vMIP-II N terminus in binding to CX3CR1 and the importance of the FKN N terminus in affinity and efficacy for CX3CR1. The data provide insights into the pharmacophore for chemokine binding to and activation of CX3CR1.

Materials and Methods

Materials. An aqueous extract of a Kaposi's sarcoma lesion was a gift from Dr. Sankar Swaminathan (University of Florida, Gainesville, FL). Oligonucleotides were purchased from Fisher Scientific (Houston, TX). Cell culture and transfection reagents were purchased from Invitrogen (Carlsbad, CA). HEK cells expressing human CCR5 were a gift from Dr. Philip Murphy (Laboratory of Host Defenses, National Institute of Allergy and Infectious Diseases, National Institutes of Health, Bethesda, MD). Ni-NTA slurry was purchased from QIAGEN (Valencia, CA). Radiolabeled ^{125}I-human SDF-1α and ^{125}I-Na were purchased from PerkinElmer Life and Analytical Sciences (Boston, MA). FKN-CD, MCP-1, MIP-1α, SDF-1α, and vMIP-II were purchased from R&D Systems (Minneapolis, MN). Fractalkine sandwich enzyme-linked immunosorbent assay kit (Quantikine DuoSet) was purchased from R&D Systems. Anti-Akt (protein kinase B) primary (Phos-Akt and Akt) and secondary antibodies were purchased from Cell Signaling Technology Inc. (Beverley, MA).

Generation of FKN and vMIP-II Mutants. The purified mammalian cell-expressed FKN used in this study has been described previously by our group as form A of FKN (Harrison et al., 2001). In brief, the molecule contains the FKN chemokine domain attached to a small portion of the mucin stalk. This sequence encoding FKN (including the signal peptide) was cloned into the mammalian cell expression vector, pcDNA3.1/myc/His6x (Invitrogen). The entire protein coding sequences of each mutated form of FKN and vMIP-II were subjected to DNA sequencing to confirm the fidelity of the DNA polymerase (*Pfu*) and to verify that the nucleotides encoding the myc/His6x were in frame with the nucleotides encoding the respective chemokines. Using site-directed, oligonucleotide-based mutagenesis, DNA sequences encoding the amino acids Asn, Ile, and Thr were each mutated to Ala in FKN to produce FKN/AAA. Using a similar method, the amino acids Asn, Ile, and Thr were deleted in FKN to produce FKNΔNIT.

DNA sequences encoding vMIP-II were isolated from an aqueous extract of a Kaposi's sarcoma lesion by polymerase chain reaction. The resulting vMIP-II DNA was cloned into the BamHI/XhoI sites of pcDNA3.1/myc/His6x (Invitrogen). Using sequential site-directed, oligonucleotide-based mutagenesis, DNA sequences encoding the amino acids Asn, Ile, and Thr were inserted between the first two cysteine residues in vMIP-II/pcDNA3.1/myc/His6x, to produce vMIP-II/N, vMIP-II/NI, and vMIP-II/NIT.

Using site-directed, oligonucleotide-based mutagenesis, the DNA sequences encoding the N-I diamino acid motif of FKN (in the pcDNA3.1/myc/His6x plasmid) were engineered to create an additional SspI cut site (AAT ATT). The SspI fragments containing the respective N-terminal portions of FKN and vMIP-II were isolated and used to replace the corresponding domains in FKN and vMIP-II to produce vMIP-II(1-9)FKN and FKN(1-12)vMIP-II. Using the DNA sequences encoding FKN, vMIP-II/NIT, vMIP-II(1-9)FKN, and FKN(1-12)vMIP-II as templates, additional mutant peptides were engineered to contain residues from both FKN and vMIP-II in their N termini. The Gly at position 4 was mutated to Arg, the Val at position 5 was mutated to Pro, and the Thr at position 6 was mutated to Asp in FKN and FKN(1-12)vMIP-II to create FKN(1-2)vMIP-II/NIT and vMIP-II(4-6)FKN, respectively. The Arg at position 7 was mutated to Gly, the Pro at position 8 was mutated to Val, and the Asp at position 9 was mutated to Thr in vMIP-II/NIT and vMIP-II(1-9)FKN to create FKN(7-9)vMIP-II/NIT, and vMIP-II(1-5)FKN, respectively.

Expression, Purification, and Western Blot Analysis of Proteins. HEK293T cells were grown to ~80% confluence in 100-mm poly-D-lysine (5 μg/ml)-coated dishes and were transfected with 10 μg of plasmid DNA and 25 μl of LipofectAMINE (Invitrogen) reagent according to the manufacturer's instructions. Cells were incubated in DMEM containing 10% FBS for the first 20 h after transfection and subsequently incubated in 8 ml of DMEM containing 0.5% FBS for an additional 24 h. Medium collected at 24, 48, and 72 h after transfection was subjected to Ni-NTA chromatography according to QIAexpressionist instructions (QIAGEN). In brief, conditioned medium pooled from eight 100-mm plates was mixed with an equal volume of 2× lysis buffer (100 mM NaH_2PO_4, 600 mM NaCl, and 20 mM imidazole, pH 8.0) and 1.5 ml of Ni-NTA resin slurry (QIAGEN). The mixture was rocked overnight at 4°C and subsequently centrifuged at 5000*g* for 5 min at RT to concentrate the slurry to 5 ml. The resulting 5 ml of slurry/medium was loaded into a gel filtration column and the packed resin bed was washed with 8 ml of wash buffer (50 mM NaH_2PO_4, 300 mM NaCl, and 20 mM imidazole, pH 8.0). The protein was eluted into 4 × 500-μl fractions with elution buffer (50 mM NaH_2PO_4, 300 mM NaCl, and 250 mM imidazole, pH 8.0), flash frozen in liquid N_2 as 100-μl aliquots, and subsequently stored at −80°C until further use. Protein aliquots were subjected to SDS-PAGE, transferred to polyvinylidene difluoride, and the membranes were incubated overnight at 4°C with anti-myc primary antibody (Invitrogen) at a 1:20,000 dilution, and subsequently incubated in sheep anti-mouse IgG/horseradish peroxidase (Invitrogen) secondary antibody at a 1:2000 dilution at RT for 1 h. Western blot analysis was used to determine the relative amounts of purified

protein contained in each Ni-NTA-eluted aliquot. Absolute values of the purified FKNs were determined by sandwich enzyme-linked immunosorbent assay, and concentrations of all other purified proteins were normalized by densitometric analysis of Western blots probed with the anti-myc epitope antibody.

Whole Cell Radioligand Binding Analysis. Procedures for radioligand binding analysis and radiolabeling of chemokines are described in detail in previously published protocols (Davis et al., 2003). CHO cells stably expressing CX3CR1, CCR2, or US28 were seeded at a density of ~300,000 cells/well into 12-well cell culture plates (Corning Glassworks, Corning, NY) with Ham's F-12 medium containing 10% FBS and 1% penicillin/streptomycin. SK-N-SH cells were seeded at a density of ~300,000 cells/well into 12-well cell culture plates with minimal essential medium-α containing 10% FBS and 0.2% penicillin/streptomycin. HEK293 cells stably expressing CCR5 were seeded into poly-D-lysine-coated 12-well cell culture plates at a density of ~300,000 cells/well with DMEM containing 10% FBS and 1% Pen/Strep. The concentrations of the radiolabeled ligands used in each competition binding analysis and the experimentally determined K_d values (mean ± S.E.M.) for each receptor are as follows: 0.2 nM ^{125}I-FKN-CD (100–300 Ci/mmol) for CX3CR1-CHO (K_d = 1.3 ± 0.3 nM) or US28-CHO (K_d = 1.7 ± 0.2 nM) cells; 0.5 nM ^{125}I-MCP-1 (100–300 Ci/mmol) for CCR2-CHO (K_d = 0.9 ± 0.2 nM) cells; 0.5 nM ^{125}I-MIP-1α (100–300 Ci/mmol) for CCR5-HEK293 (K_d = 1.7 ± 0.1 nM) cells; and 20 pM ^{125}I-SDF-1α (2200 Ci/mmol; PerkinElmer Life and Analytical Sciences) for CXCR4 on SK-N-SH cells (K_d = 5.0 ± 0.8 nM). Nonspecific binding was determined in the presence of 100 nM unlabeled FKN-CD for CX3CR1 and US28, MCP-1 for CCR2, MIP-1β for CCR5, and SDF-1α for CXCR4.

Western Blot Analysis of FKN-Stimulated Akt Phosphorylation. Wild-type CHO cells, or CHO cells stably expressing CX3CR1 were plated into 12-well cell culture dishes and allowed to grow 48 h to 70 to 90% confluence. Just before stimulation, cells were incubated in serum-free Ham's F-12 medium for 2 h. Cells were then incubated in serum-free Ham's F-12 containing various concentrations of purified proteins in a total reaction volume of 200 μl per well. After stimulation, medium was aspirated, the plates were placed directly on ice, and then each well was washed one time with ice-cold phosphate-buffered saline. Cells were collected in 100 μl of 1× Laemmli sample buffer containing 3% β-mercaptoethanol and sonicated 5 to 10 s on ice to shear DNA and reduce sample viscosity. Samples were boiled for 5 min and centrifuged at 10,000*g* for 1 min. At this point, the samples were frozen at −20°C until further use, or 40 μl of sample was immediately subjected to SDS-PAGE and Western blot analysis. Membranes (polyvinylidene difluoride) were incubated overnight at 4°C in anti-phos-Akt antibody (Cell Signaling Technology Inc.) at a 1:1000 dilution and subsequently incubated in goat anti-rabbit IgG/horseradish peroxidase secondary antibody (Cell Signaling Technology Inc.) at a 1:2000 dilution at RT for 1 h. To strip anti-Phos-Akt antibody, membranes were incubated in stripping buffer (25 mM glycine-HCl, pH 2.0, and 1% SDS) for 30 min at 65°C. After stripping, membranes were incubated in anti-Akt antibody (Cell Signaling Technology Inc., Minneapolis, MN) at a 1:2000 dilution overnight at 4°C. Maximal stimulation of Phos-Akt by FKN-CD occurred at time points of 5 and 10 min (data not shown). Thus, in all functional experiments a time point of 7 min was used.

Data Analysis. Graphs and statistical analysis were performed using Prism and InStat from GraphPad Software Inc. (San Diego, CA). Competitive binding data were analyzed with Prism and IC_{50} values were converted to K_i values (using experimentally determined K_d values of the radioligand) by using the Cheng-Prusoff equation (Cheng and Prusoff, 1973). Statistical analysis was performed using analysis of variance followed by a Dunnett's multiple comparisons test (Fig. 6) or using Student's *t* test (Table 1 and 2). The level of statistically significant difference was defined as $p < 0.05$.

Results

Figure 1, top, depicts an amino acid alignment of the chemokine domain of human FKN compared with *Human herpesvirus 8* vMIP-II. Whereas the sequences of the two chemokines contain many identical amino acids, the most notable difference is the three amino acids (X3 bulge) that lie between the first two conserved cysteine residues in FKN. Modified forms of either FKN or vMIP-II were created to assess the role of the X3 bulge (NIT) in the affinity, efficacy, and selectivity of FKN at its receptor CX3CR1. Additional FKN/vMIP-II chimeras were generated to evaluate the role of the N-terminal segments of these chemokines in the CX3CR1 binding and activation properties. Figure 1, bottom, highlights the various mutated and chimeric proteins as they relate to the FKN and vMIP-II sequences. HEK293T cells were engineered to express each of the 11 peptides shown in Fig. 1. Conditioned media from the transfected cells were collected, and the secreted proteins were purified by Ni-NTA chromatography and subsequently characterized in binding and functional assays.

```
                      1   2                          3
huFKN-CD      QHHGVTKCNITCSKMT SKIPVALLIH YQQNQASCGK
 vMIP-II  LGASWHRPDKC   CLGYQKRPLPQVLLSSWYPTSQ LCSK
                          4
huFKN-CD RAIILETRQH RLFCADPKEQ WVKDAMQHLD RQAAALTRNG
 vMIP-II PGVIFL TKRGRQVCAD KSKDWVKKLMQQLP  VTAR
```

```
                          1   2
          FKN/AAA      QHHGVTKCAAACSKMT SKIPVALLIH...
          FKNΔNIT      QHHGVTKC   CSKMT SKIPVALLIH...
       vMIP-II/NIT  LGASWHRPDKCNITCLGYQKRPLPQVLLSS...
  FKN(1-12)vMIP-II     QHHGVTKCNITCLGYQKRPLPQVLLSS...
   vMIP-II(1-9)FKN  LGASWHRPDKCNITCSKMT SKIPVALLIH...
   vMIP-II(1-5)FKN  LGASWHGVTKCNITCSKMT SKIPVALLIH...
FKN(1-2)vMIP-II/NIT     QHHRPDKCNITCLGYQKRPLPQVLLSS...
  FKN(3-12)vMIP-II  LGASWHGVTKCNITCLGYQKRPLPQVLLSS...
   vMIP-II(4-6)FKN      QHHRPDKCNITCSKMT SKIPVALLIH...
```

Fig. 1. Alignment of FKN, vMIP-II, and chimera amino acid sequences. Alignment was achieved using the PILEUP algorithm of GCG. Top, mature forms of the FKN and vMIP-II are shown. The four conserved cysteine residues are indicated numerically (1–4). The X3 bulge of FKN and the conserved cysteine residues are bold typed and the α-helix of FKN is underlined. Bottom, sequences of each of the nine mutant forms of FKN and vMIP-II are indicated. The NIT of vMIP-II/NIT and the AAA of FKN/AAA are bold typed and blue. In the present study, the residues up to and including the second conserved cysteine are considered to be the N terminus of each peptide. The residues from FKN are indicated in green, and the residues from vMIP-II are indicated in red.

Generation of FKN with a Modified X3 Bulge That Retains Affinity and Efficacy for CX3CR1 and a CC Form of FKN with Reduced Affinity for CX3CR1. The amino acids Asn, Ile, and Thr that lie between the first two conserved Cys residues were each mutated to Ala, to create a molecule termed FKN/AAA (Fig. 1), and the "NIT" was deleted to create a CC form of FKN, termed FKNΔNIT (Fig. 1). Figure 2A depicts Western blot analyses of the HEK293T cell-expressed and Ni-NTA-purified FKN, FKN/AAA, and FKNΔNIT. FKN migrated as a diffuse band at a relative molecular mass (M_r) greater than what was predicted based on the protein backbone. This is consistent with previous results published by our group (Harrison et al., 2001) and is probably a result of the glycosylation of either the NIT and/or the mucin stalk (the secreted FKN protein is expressed attached to a small portion of the mucin stalk; see *Materials and Methods*). The FKN/AAA and FKNΔNIT molecules migrated at M_r values slightly lower than FKN, yet higher than their predicted M_r values. This is probably a result of elimination of the *N*-linked glycosylation consensus sequence. Figure 2B indicates that the three chemokine peptides bind CX3CR1 with a rank order of potency FKN = FKN/AAA > FKNΔNIT. The HEK293T-expressed FKN bound to CX3CR1 with a calculated K_i (±S.E.M.) of 1.7 ± 0.3 nM, which is similar to the K_i value determined for FKN/AAA of 1.9 ± 0.8 nM. The deletion of the NIT disrupts the ability of FKN to bind its receptor, as evidenced by the inability of FKNΔNIT to significantly compete for radiolabeled FKN-CD binding over the range of concentrations tested.

Purified FKN/AAA stimulated Phos-Akt in a concentration-dependent manner in CX3CR1-CHO cells. Figure 2C shows representative Western blots, and Fig. 2D summarizes results from three independent experiments indicating FKN/AAA stimulated Phos-Akt in the CHO-CX3CR1 cells with the same potency and efficacy as FKN.

Generation of a CX3C Form of vMIP-II with Enhanced Affinity for CX3CR1 and Reduced Affinity for CCR2,

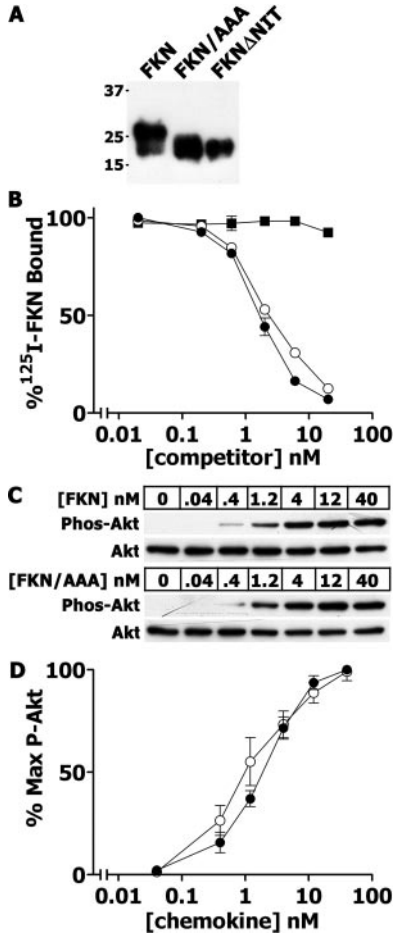

Fig. 2. An X3 bulge modified form of FKN (FKN/AAA) retains affinity and efficacy for CX3CR1. A, aliquots (1 μl) of the normalized purified proteins were subjected to SDS-PAGE and Western blot analysis using the anti-myc antibody. B, competitive binding of ^{125}I-huFKN-CD (0.2 nM) to CHO cells stably expressing huCX3CR1 in the presence of increasing concentrations of FKN (●), FKN/AAA (○), and FKNΔNIT (■). Results are expressed as a mean ± S.E.M. from three independent experiments performed in triplicate. C, representative Western blot analysis depicting concentration-dependent stimulation of Phos-Akt by FKN and FKN/AAA purified proteins on huCX3CR1-CHO cells. D, concentration-response curves are plotted as a mean ± S.E.M. from three independent experiments performed in triplicate. Relative Phos-Akt staining is plotted as a function of the concentration of FKN (●) or FKN/AAA (○).

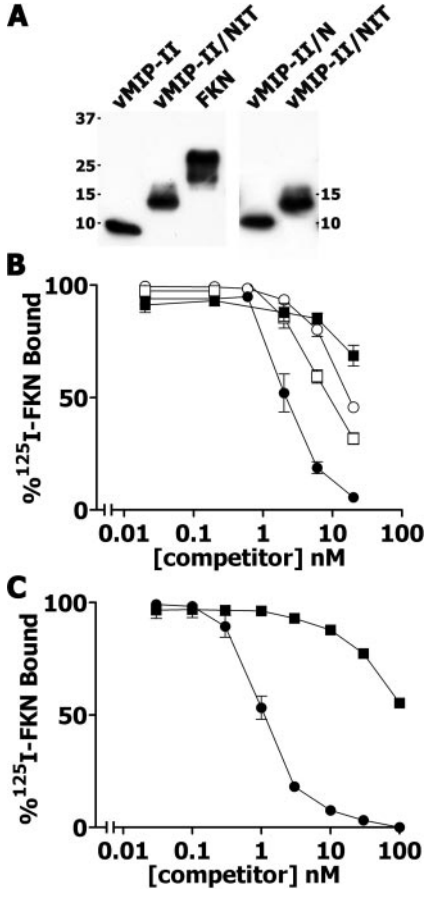

Fig. 3. An X3 bulge modified form of vMIP-II (vMIP-II/NIT) has enhanced affinity for CX3CR1. A, aliquots (1 μl) of the normalized Ni-NTA purified proteins were subjected to SDS-PAGE and Western blot analysis using the anti-myc antibody. B, competitive binding of ^{125}I-huFKN-CD (0.2 nM) to huCX3CR1-CHO cells in the presence of increasing concentrations of FKN (●), vMIP-II/NIT (□), vMIP-II/N (○), and vMIP-II (■). Results are expressed as a mean ± S.E.M. from three or six independent experiments performed in triplicate. Calculated K_i values (± S.E.M.) for FKN and vMIP-II/NIT are 1.7 ± 0.3 and 7.9 ± 0.7 nM, respectively. C, competitive binding of ^{125}I-huFKN-CD (0.2 nM) to huCX3CR1-CHO cells in the presence of increasing concentrations of commercially available (R&D Systems) huFKN-CD (●) and vMIP-II (■). Results are expressed as a mean ± S.E.M. from three independent experiments performed in triplicate. Calculated K_i values (± S.E.M.) for commercially available huFKN-CD and vMIP-II are 0.9 ± 0.1 and 112 ± 6 nM, respectively.

TABLE 1

Calculated K_i values of FKN, vMIP-II, and vMIP-II/NIT at CX3CR1, CCR2, CCR5, CXCR4, and US28

Competition binding of expressed proteins at each of the receptors is described under *Materials and Methods*. IC_{50} values were converted to K_i values (using experimentally determined K_d values of the radioligand) by using the Cheng-Prusoff equation. K_i values are expressed as mean ± S.E.M. from three to six independent experiments performed in triplicate.

Receptor	K_i		
	FKN	vMIP-II	vMIP-II/NIT
		nM	
CX3CR1	1.7 ± 0.3	>53	7.9 ± 0.7*[a]
CCR2	N.D.	1.0 ± 0.1	24.0 ± 4.9*[bc]
CCR5	N.D.	3.0 ± 0.7	>131
CXCR4	N.D.	20 ± 6.2	>286
US28	2.9 ± 0.8	1.1 ± 0.5	2.6 ± 1.2

N.D., not determined
* $p < 0.05$.
[a] Comparing FKN with vMIP-II/NIT at CX3CR1.
[b] Comparing vMIP-II with vMIP-II/NIT at CCR2.
[c] Comparing vMIP-II/NIT at CCR2 with vMIP-II/NIT at CX3CR1.

CCR5, CXCR4, and US28. Using site-directed insertional mutagenesis, the amino acids Asn, Ile, and Thr were introduced sequentially into the vMIP-II sequence between the first two cysteine residues to create vMIP-II/NIT. Figure 3A depicts anti-myc Western blot analyses of the HEK293T cell-expressed and Ni-NTA-purified FKN, vMIP-II, vMIP-II/N, and vMIP-II/NIT proteins. The mature vMIP-II protein is composed of 76 amino acids and thus the observed 8-kDa protein is consistent with its predicted M_r. vMIP-II/NIT migrated with an apparent molecular mass of 14 kDa. The larger than expected size difference between vMIP-II and vMIP-II/NIT could be accounted for by glycosylation of this sequence. Figure 3B indicates that the four chemokine peptides bind CX3CR1 with a rank order of potency, FKN > vMIP-II/NIT > vMIP-II/N > vMIP-II. The HEK293T-expressed FKN bound to CX3CR1 with a calculated K_i (± S.E.M.) of 1.7 ± 0.3 nM, which is similar to the K_i value (K_i = 0.9 ± 0.1 nM) determined using commercially available FKN-CD (Fig. 3C). Likewise, HEK293T-expressed vMIP-II and commercially available vMIP-II displayed equivalent affinities for CX3CR1 (Fig. 3, B and C). These results indicated that the binding properties of the mammalian cell-expressed purified proteins and commercially available proteins are comparable. vMIP-II/NIT binds CX3CR1 with an approximate 4-fold lower affinity than FKN (calculated K_i = 7.9 ± 0.7 nM), and about a 10-fold higher affinity compared with vMIP-II (Table 1).

vMIP-II is known to bind several CC and CXC chemokine receptors. The purified HEK293T-expressed vMIP-II and vMIP-II/NIT proteins were characterized in a series of competition binding experiments at CCR2, CCR5, and CXCR4. vMIP-II competed for ^{125}I-huMCP-1 (0.2 nM) binding to huCCR2-CHO cells (Fig. 4A), ^{125}I-huMIP-1α (0.5 nM) binding to huCCR5-HEK cells (Fig. 4B), and ^{125}I-huSDF-1α (20 pM) binding to CXCR4-expressing SK-N-SH cells (Fig. 4C) with measurable potencies. The addition of the NIT into the vMIP-II protein yielded a molecule with reduced affinity for CCR2, CCR5, and CXCR4 (Table 1).

Multiple studies have shown that FKN and vMIP-II bind human cytomegalovirus-encoded US28 with nanomolar affinities (Kledal et al., 1997, 1998; Mizoue et al., 2001). HEK293T-expressed vMIP-II and commercially available vMIP-II display approximately equal affinities for US28 binding with a K_i (± S.E.M.) of 1.1 ± 0.5 and 2.1 ± 0.6 nM, respectively (Fig. 5, A and B). Interestingly, commercially available FKN-CD binds US28 with a K_i of 0.1 ± 0.01 nM, whereas the purified HEK293T-expressed FKN (containing a portion of the mucin stalk) binds with a K_i of 2.9 ± 0.8 nM. vMIP-II/NIT bound to US28 with a K_i of 2.6 ± 1.2 nM. The addition of the NIT into vMIP-II reduces the affinity of vMIP-II for US28 approximately 2-fold, although this difference was not statistically significant (Table 1).

Antagonism of FKN-Induced Akt Phosphorylation by vMIP-II/NIT. Figure 6A shows the effects of purified FKN (at a concentration that produced maximal stimulation) and increasing concentrations of purified vMIP-II, and vMIP-II/NIT on Phos-Akt stimulation in CX3CR1-CHO cells. The vMIP-II and vMIP-II/NIT proteins stimulated a very low level of Phos-Akt in the CX3CR1-expressing CHO cells (Fig. 6A). FKN, vMIP-II, and vMIP-II/NIT did not stimulate Phos-Akt in wild-type CHO cells (data not shown).

Because vMIP-II and vMIP-II/NIT did not display significant agonist activity, and given that vMIP-II has been reported to be a CX3CR1 antagonist, the ability of vMIP-II and vMIP-II/NIT to inhibit FKN-induced Phos-Akt was evaluated. Figure 6B shows a representative Western blot depicting FKN-stimulated Phos-Akt in the absence and presence of a fixed concentration of either vMIP-II or vMIP-II/NIT.

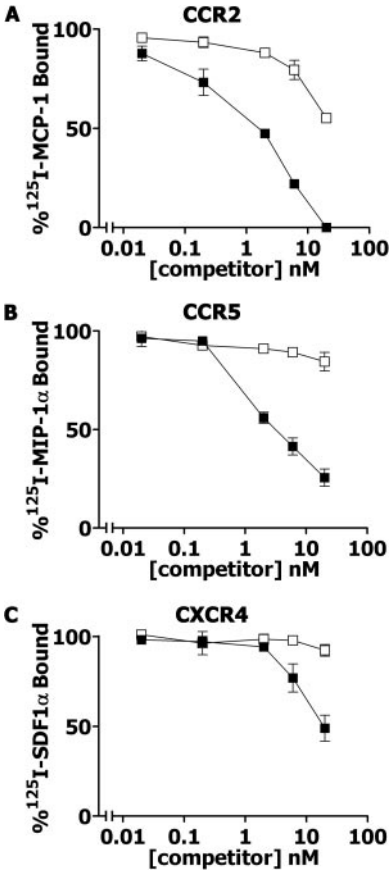

Fig. 4. vMIP-II/NIT has a lower affinity for CCR2, CCR5, and CXCR4 compared with vMIP-II. Binding data are plotted as percentage bound of the labeled chemokines as a function of the concentration of vMIP-II (■) or vMIP-II/NIT (□). Results are expressed as a mean ± S.E.M. from three independent experiments performed in triplicate. Calculated vMIP-II K_i values (± S.E.M.) are indicated. A, ^{125}I-huMCP-1 (0.5 nM) binding to CHO cells stably expressing huCCR2 (vMIP-II K_i = 1.0 ± 0.1 nM). B, ^{125}I-huMIP-1α (0.5 nM) binding to HEK293 cells stably expressing huCCR5 (vMIP-II K_i = 3.0 ± 0.7 nM). C, ^{125}I-huSDF-1α (20 pM) binding to SK-N-SH cells (vMIP-II K_i = 20 ± 6.2 nM).

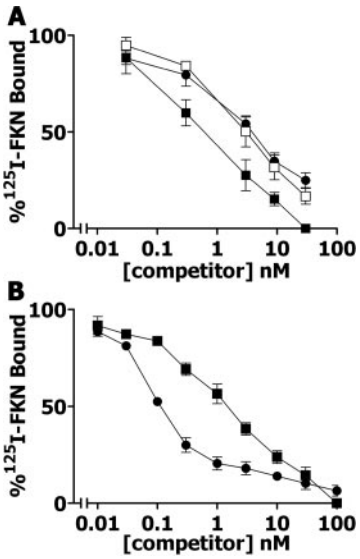

Fig. 5. vMIP-II/NIT binds to the virally-encoded chemokine receptor US28. Competitive binding of ^{125}I-huFKN-CD (0.2 nM) to CHO cells stably expressing US28 in the presence of FKN, vMIP-II, and vMIP-II/NIT. Results are expressed as a mean ± S.E.M. from three independent experiments. A, competitive binding of FKN (●), vMIP-II (■), and vMIP-II/NIT (□). Calculated K_i values (± S.E.M.) for FKN, vMIP-II, and vMIP-II/NIT are 2.9 ± 0.8, 1.1 ± 0.5, and 2.6 ± 1.2 nM, respectively. B, competitive binding of commercially available (R&D Systems) huFKN-CD (●) and vMIP-II (■). Calculated K_i values (± S.E.M.) for commercially available huFKN-CD and vMIP-II are 0.1 ± 0.01 and 2.1 ± 0.6 nM, respectively.

FKN-CD stimulated Phos-Akt in CX3CR1-CHO cells in a concentration-dependent manner. In the presence of 40 nM vMIP-II, activation by FKN-CD was not affected. However, in the presence of 40 nM vMIP-II/NIT, stimulation of Phos-Akt by FKN-CD was inhibited. Figure 6C summarizes results from three independent experiments. In the presence of vMIP-II/NIT, the FKN-CD concentration-dependent stimulation of Phos-Akt was right-shifted compared with stimulation of Phos-Akt in the presence of FKN-CD alone. These data are consistent with vMIP-II/NIT acting as an inhibitor of FKN-stimulated CX3CR1 signaling.

Role of N Terminus of FKN and vMIP-II in the Affinity and Efficacy for CX3CR1. Two chimeric proteins were generated in which the N terminus of FKN was replaced with the first five or nine amino acids of vMIP-II to create vMIP-II(1-5)FKN and vMIP-II(1-9)FKN (Fig. 1). These two peptides competed weakly with ^{125}I-huFKN-CD (0.2 nM) for binding to huCX3CR1 (Fig. 7A); their affinities for CX3CR1 were reduced by approximately 100-fold (Table 2). Neither vMIP-II(1-5)FKN nor vMIP-II(1-9)FKN stimulated Phos-Akt in CX3CR1-expressing CHO cells (data not shown). To contrast, replacement of the N terminus of vMIP-II with the corresponding domain of FKN yielded a molecule with high affinity and efficacy for CX3CR1. The FKN(1-12)vMIP-II chimeric protein bound to CX3CR1 (Fig. 7B) and stimulated Phos-Akt in the CHO-CX3CR1 cells (Fig. 7, C and D) with the same potency as FKN. FKN(1-12)vMIP-II did not stimulate Phos-Akt in wild-type CHO cells (data not shown).

To further elucidate the roles of specific amino acids within the FKN N terminus necessary for high-affinity binding and activation of CX3CR1, an additional series of chimeric peptides were generated. FKN and vMIP-II molecules were created that contained residues from both FKN and vMIP-II within their respective N termini (Fig. 1). Each of the peptides competed with ^{125}I-huFKN-CD (0.2 nM) for binding to huCX3CR1 (Fig. 8A and calculated K_i values shown in Table 2). In addition, each peptide displayed varying levels of activity in stimulating Phos-Akt in CX3CR1-expressing cells. FKN(1-2)vMIP-II/NIT was indistinguishable from vMIP-II/NIT in its ability to bind (K_i = 6.0 ± 1.3 nM) and had no agonist activity at CX3CR1. On the other hand, vMIP-II(4-6)FKN (K_i = 4.0 ± 0.7 nM) and FKN(3-12)vMIP-II (K_i = 2.1 ± 0.2 nM) had slightly higher affinity for CX3CR1 compared with vMIP-II/NIT. In addition, each of these peptides displayed some agonist activity.

Discussion

Structural studies have indicated that the CX3C sequence of FKN forms a bulge in the N terminus that is not seen in other families of chemokines (Mizoue et al., 1999; Hoover et al., 2000). Our data indicate the X3-bulge is an important determinant in the high affinity of FKN for CX3CR1 and suggest that the X3 bulge acts only as a structural spacer. The CX3C sequences of both human and rat FKN contain Asn-Ile-Thr (NIT) between the first two cysteines, whereas the murine FKN contains Glu-Ile-Met (EIM). This triamino acid motif of human and rat FKN (NIT) forms a potential *N*-linked glycosylation site. In our previous study, we reported that the X3 bulge of human FKN was probably not glycosylated, as evidenced by an apparent lack in electrophoretic mobility shift in SDS-PAGE when comparing wild-type FKN to the EIM mutant. However, it was probable that a small increase in mass caused by potential *N*-linked glycosylation was masked by the relatively high molecular mass of the form of FKN used in those experiments (i.e., FKN-CD with the entire mucin stalk). Because the FKN used in this

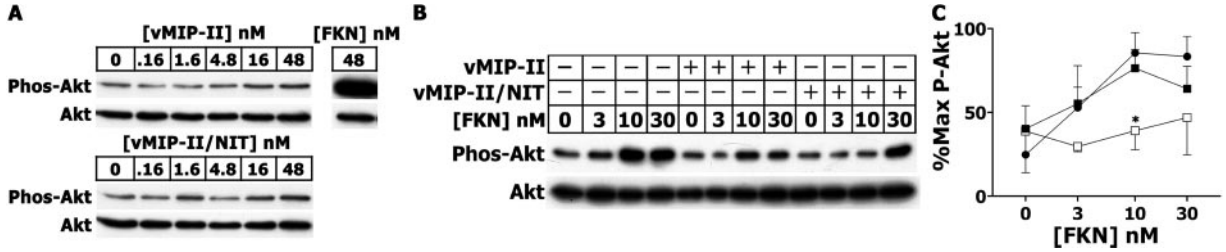

Fig. 6. Effects of FKN, vMIP-II, and vMIP-II/NIT on Akt phosphorylation in CX3CR1-expressing CHO cells. A, effects of FKN, vMIP-II, and vMIP-II/NIT on Phos-Akt in CHO cells stably expressing CX3CR1. Autoradiographs of Western blot analysis are shown as a representative result of three independent experiments. B, vMIP-II and vMIP-II/NIT proteins (40 nM) were added in the presence of increasing concentrations of huFKN-CD. B, huFKN-CD concentration-response curves are plotted as a mean ± S.E.M. from three independent experiments (*, $p < 0.05$). Relative Phos-Akt staining was normalized to total-Akt staining and plotted as a function of huFKN-CD concentration in the absence of (●) or presence of a fixed concentration (40 nM) of either vMIP-II (■) or vMIP-II/NIT (□).

study migrates at a lower molecular mass (25–30 kDa), because of the shorter mucin stalk, we observed a mobility shift between wild-type FKN and the FKN/AAA mutant. The enhanced electrophoretic mobility of the latter protein is probably a consequence of a lack in *N*-linked glycosylation. Variants of human FKN in which the NIT was replaced by EIM, AIT, or AAA bound and stimulated CX3CR1 similar to wild-type human FKN (Harrison et al., 2001; Mizoue et al., 2001; current study). Thus, the specific amino acids in these positions do not play a role in the ability of FKN to bind and activate the receptor.

A role of the X3 bulge in affinity for CX3CR1 also comes from results characterizing a CX3C form of vMIP-II, because vMIP-II/NIT bound with higher affinity than either vMIP-II/N or vMIP-II. Whereas the X3 bulge enhanced the affinity of vMIP-II for CX3CR1, it is not the only determinant, because vMIP-II/NIT did not bind with an affinity equal to that of FKN. The CNIC variant (i.e., a CX2C form of vMIP-II) did not express in our mammalian cell culture system (data not shown), and as a consequence, only vMIP-II/N and vMIP-II/NIT were tested for their affinities at CX3CR1. It has been hypothesized that because of structural constraints enforced by the first cysteine disulfide bridge, only chemokines containing none, one, or three amino acids between the first two cysteines could exist (Rollins, 1997). Thus, the inability to express a CX2C form of vMIP-II could be explained by this original hypothesis.

The X3-bulge is also a key determinant of the selectivity of FKN for CX3CR1 because vMIP-II/NIT had a lower affinity for CCR2, CCR5, and CXCR4 compared with vMIP-II. To assess the affinity of vMIP-II/NIT for the virally encoded chemokine receptor US28, we compared the binding of purified FKN, vMIP-II, and vMIP-II/NIT to commercially available FKN-CD and vMIP-II. Multiple studies have shown that FKN and vMIP-II bind US28 with nanomolar affinity (Kledal

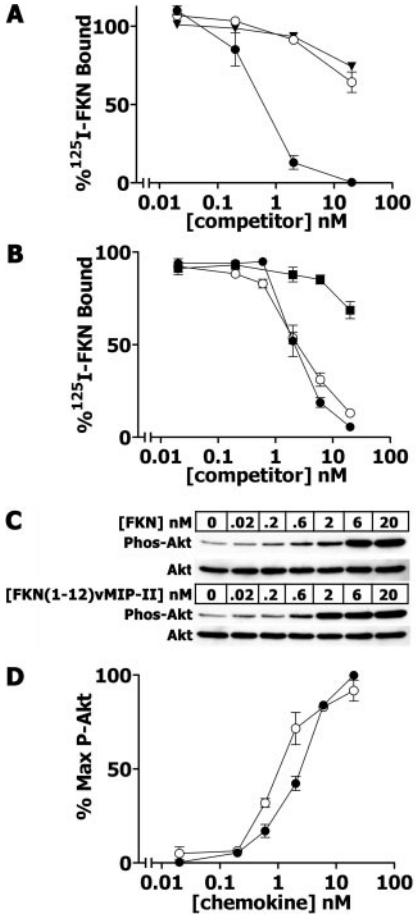

Fig. 7. The N termini of FKN and vMIP-II determine affinity and efficacy at CX3CR1. A, competitive binding of ^{125}I-huFKN-CD (0.2 nM) to CHO cells stably expressing huCX3CR1 in the presence of increasing concentrations of FKN (●), vMIP-II(1–5)FKN (▼), and vMIP-II(1–9)FKN (○). Results are expressed as a mean ± S.E.M. from three independent experiments performed in triplicate. B, competitive binding of ^{125}I-huFKN-CD (0.2 nM) to CHO cells stably expressing huCX3CR1 in the presence of increasing concentrations of FKN (●), vMIP-II (■), and FKN(1-12)vMIP-II (○). Results are expressed as a mean ± S.E.M. from three independent experiments performed in triplicate. C, representative Western blot depicting concentration-dependent stimulation of Phos-Akt by FKN and FKN(1-12)vMIP-II in huCX3CR1-expressing CHO cells. D, concentration-response curves are plotted as a mean ± S.E.M. from three independent experiments performed in triplicate. Relative Phos-Akt staining is plotted as a function of the concentration of FKN (●) or FKN(1-12)vMIP-II (○).

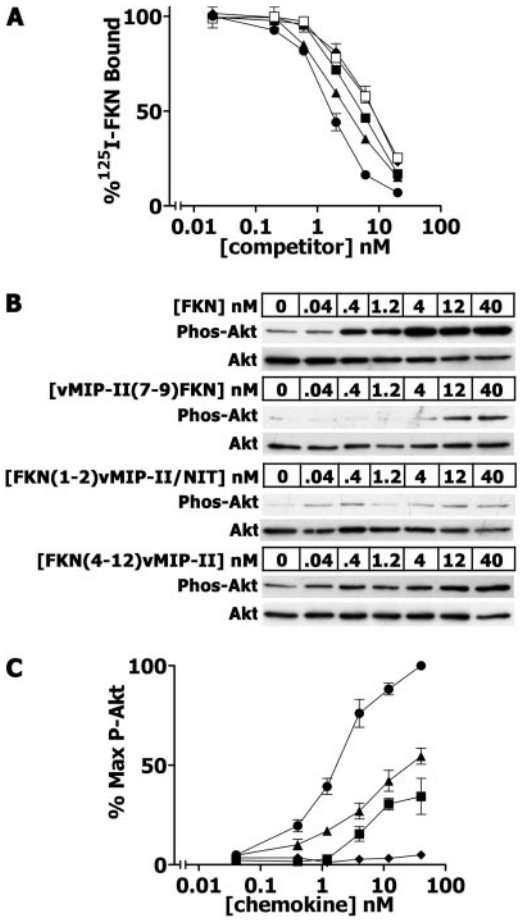

Fig. 8. The entire N terminus of FKN is necessary for high affinity and full efficacy at CX3CR1. A, competitive binding of ^{125}I-huFKN-CD (0.2 nM) to huCX3CR1-CHO cells in the presence of increasing concentrations of FKN (●), vMIP-II/NIT (□), FKN(1-2)vMIP-II/NIT (diamonds), vMIP-II(4-6)FKN (■), and FKN(7-9)vMIP-II/NIT (triangles). Results are expressed as a mean ± S.E.M. from three independent experiments performed in triplicate. B, representative Western blots depicting concentration-dependent stimulation of Phos-Akt by FKN, FKN(1-2)vMIP-II/NIT, vMIP-II(4-6)FKN, and FKN(3-12)vMIP-II on huCX3CR1-expressing CHO cells. C, concentration-response curves are plotted as a mean ± S.E.M. from three independent experiments performed in triplicate. Relative Phos-Akt staining is plotted as a function of the concentration of FKN (●), FKN(1-2)vMIP-II/NIT (◆), vMIP-II(4-6)FKN (■), and FKN(3-12)vMIP-II (▲).

et al., 1997, 1998; Mizoue et al., 2001). Furthermore, Kledal et al. (1998) demonstrated that the affinity of secreted FKN-CD attached to the mucin stalk is approximately 7 times lower than the affinity for the FKN-CD alone determined in competition against ^{125}I-FKN-CD. The purified FKN used in this study contains a small portion of the mucin stalk, and this probably explains why the FKN had a lower affinity for US28 compared with FKN-CD. Despite the fact that US28 binds FKN, the lower affinity of vMIP-II/NIT at US28 suggests that this virally encoded chemokine binds US28 in a manner different from the way in which it binds CX3CR1.

In the present study, the phosphatidylinositol 3-kinase-dependent phosphorylation of Akt was used a measure of receptor activation. This pathway is known to play a role in FKN-induced chemotaxis and cell survival (Boehme et al., 2000; Meucci et al., 2000; Kansra et al., 2001). FKN stimulated Akt phosphorylation in a robust manner, whereas vMIP-II and vMIP-II/NIT displayed some partial, albeit minimal, agonist activity at CX3CR1. These findings are not inconsistent with previous reports of the antagonistic effects of vMIP-II at CX3CR1 (Chen et al., 1998), and indicate that the addition of the NIT into vMIP-II/NIT has not converted the molecule into a full agonist. In the presence of a half-maximal concentration, vMIP-II/NIT antagonized FKN-stimulated phosphorylation of Akt. The greater ability of vMIP-II/NIT, compared with vMIP-II, to antagonize FKN-stimulated CX3CR1 signaling is consistent with the binding data as vMIP-II/NIT has the higher affinity for CX3CR1. Using the virally encoded nonselective antagonist as a template and modifying it in a manner that changes its receptor selectivity could allow development of chemokine receptor antagonists that may prove useful in defining roles of specific chemokine/receptor interactions in health and disease.

The FKN and vMIP-II N termini are disordered in their solution structures and most likely become ordered only upon receptor binding (Liwang et al., 1999; Mizoue et al., 1999). Two studies point to key residues in the FKN-CD and N terminus important for high-affinity binding to and activation of CX3CR1 (Harrison et al., 2001; Mizoue et al., 2001). In addition, removal of the FKN N terminus caused a reduction of affinity by greater than 100-fold and produced a molecule that was unable to induce chemotaxis or calcium transients in CX3CR1-expressing cells (Mizoue et al., 2001). Multiple studies have shown that peptides composed of only the N terminus of vMIP-II bind CXCR4 (but not CCR5) and are potent CXCR4 antagonists (Luo et al., 2000; Zhou et al., 2000; Crump et al., 2001). In the present study, we report the importance of the FKN and vMIP-II N termini on the binding to and activation of CX3CR1. The addition of only the first 11 amino acids of the mature form of FKN converted vMIP-II into a molecule that had the same affinity and efficacy for CX3CR1 as FKN. Conversely, replacement of the first two amino acids of FKN with the first five residues in vMIP-II converted FKN into a peptide with low affinity for CX3CR1. These data suggest that the residues in the N termini of FKN and vMIP-II determine the affinity and efficacy at CX3CR1. However, other regions of these chemokines must also contribute to the pharmacological properties as two chimeric molecules [FKN(1-2)vMIP-II/NIT and vMIP-II(4-6)FKN] having identical N termini (QHHRPD) displayed differences in efficacy. To our surprise, FKN(3-12)vMIP-II had high affinity and significant agonist activity. Based on the results of the other chimeric molecules, it was expected that FKN(3-12)vMIP-II would have no agonist activity. These data suggest that the mechanism by which this chimeric molecule activates CX3CR1 is different from FKN or the other agonist peptides.

TABLE 2

Calculated K_i values of FKN and vMIP-II N-terminal chimeric peptides at CX3CR1

Competition binding of expressed proteins is described under *Materials and Methods* section. IC_{50} values were converted to K_i values (using experimentally determined K_d values of the radioligand) by using the Cheng-Prusoff equation. K_i values are expressed as mean ± S.E.M. from three independent experiments performed in triplicate.

Peptide	K_i at CX3CR1
	nM
FKN	1.7 ± 0.3
FKN/AAA	1.9 ± 0.8
vMIP-II/NIT	7.9 ± 0.7
FKN(1-12)vMIP-II	1.6 ± 0.7
vMIP-II(1-9)FKN	>68
vMIP-II(1-5)FKN	>73
FKN(1-2)vMIP-II/NIT	6.0 ± 1.3
vMIP-II(4-6)FKN	4.0 ± 0.7*[ab]
FKN(3-12)vMIP-II	2.1 ± 0.2*[b]

* $p < 0.05$.
[a] Compared with FKN.
[b] Compared with vMIP-II/NIT.

FKN and its receptor CX3CR1 have been implicated in a number of inflammatory mechanisms. Proinflammatory induced FKN expression probably mediates leukocyte recruitment from the blood into the interstitial tissue. Up-regulation of FKN on endothelial cells is found in inflammatory diseases, including crescentic glomerulonephritis, atherosclerosis, cutaneous inflammatory disease, and Crohn's disease (for review, see Zujovic and Harrison, 2003). FKN and CX3CR1 expression is increased in T-helper 1-associated pathologies, including psoriasis, *Mycobacterium tuberculosis* (Fraticelli et al., 2001), and cardiac allograft rejection (Robinson et al., 2000). Robinson et al. (2000) identified CX3CR1 expressing leukocytes within rejecting allografts and demonstrated increased FKN expression on rejecting mouse cardiac allografts. In addition, anti-CX3CR1 antibody significantly prolonged survival of mouse cardiac allografts in a model of acute rejection. Further support for a role of FKN/CX3CR1 in cardiac allograft rejection has come from analysis of mice lacking the gene for CX3CR1. Immunosuppressed CX3CR1$^{(-/-)}$ mice had a dramatic prolongation in allograft survival time (Haskell et al., 2001). CX3CR1$^{(-/-)}$ mice crossed into the ApoE$^{(-/-)}$ background also showed significant reductions in atherosclerotic lesion size and reduced macrophage infiltration, highlighting the importance of CX3CR1 in this disease (Combadiere et al., 2003; Lesnick et al., 2003). Furthermore, human variants of CX3CR1 have been identified and are associated with reduced risk or severity of cardiovascular disease (McDermott et al., 2001; Moatti et al., 2001; McDermott et al., 2003). The development of selective CX3CR1 antagonists (e.g., vMIP-II/NIT) will afford alternative pharmacological approaches to understanding roles for FKN and CX3CR1 in physiological and pathological scenarios that could lead to promising new therapeutics for the treatment of atherosclerosis or cardiac transplantation rejection.

In conclusion, the CX3C bulge of FKN is a major determinant of affinity and selectivity for its receptor. Similar to other chemokines, the N terminus is a defining feature of FKN, conferring the agonist properties of this chemokine. By

using a virally encoded nonselective chemokine antagonist as a template, a high-affinity selective chemokine antagonist was generated. Defining roles of specific chemokines and their receptors in either physiological or pathological scenarios has been hampered by the redundancy of their actions and the lack of selective pharmacological agents. The development of specific chemokine receptor antagonists (based upon virally encoded chemokine peptides) offers the potential for improved strategies for targeting inflammatory mechanisms associated with human disease.

Acknowledgments

We acknowledge Defang Luo and Xiaolei Qiu for technical assistance. We appreciate the generous gifts from Dr. Sankar Swaminathan (Kaposi's sarcoma lesion extract) and Dr. Philip Murphy (CCR5-expressing HEK cells).

References

Bazan JF, Bacon KB, Hardiman G, Wang W, Soo K, Rossi D, Greaves DR, Zlotnik A, and Schall TJ (1997) A new class of membrane-bound chemokine with a CX3C motif. *Nature (Lond)* **385:**640–644.

Boehme SA, Lio FM, Maciejewski-Lenoir D, Bacon KB, and Conlon PJ (2000) The chemokine fractalkine inhibits Fas-mediated cell death of brain microglia. *J Immunol* **165:**397–403.

Chen S, Bacon KB, Li L, Garcia GE, Xia Y, Lo D, Thompson DA, Siani MA, Yamamoto T, Harrison JK, et al. (1998) In vivo inhibition of CC and CX3C chemokine-induced leukocyte infiltration and attenuation of glomerulonephritis in Wistar-Kyoto (WKY) rats by VMIP-II. *J Exp Med* **188:**193–198.

Cheng Y and Prusoff WH (1973) Relationship between the inhibition constant (K1) and the concentration of inhibitor which causes 50 per cent inhibition (I50) of an enzymatic reaction. *Biochem Pharmacol* **22:**3099–3108.

Combadiere C, Potteaux S, Gao JL, Esposito B, Casanova S, Lee EJ, Debre P, Tedgui A, Murphy PM, and Mallat Z (2003) Decreased atherosclerotic lesion formation in CX3CR1/apolipoprotein E double knockout mice. *Circulation* **107:**1009–1016.

Crump MP, Elisseeva E, Gong J, Clark-Lewis I, and Sykes BD (2001) Structure/function of human herpesvirus-8 MIP-II (1-71) and the antagonist n-terminal segment (1-10). *FEBS Lett* **489:**171–175.

Davis CN, Chen S, Boehme SA, Bacon KB, and Harrison JK (2003) Chemokine receptor binding and signal transduction in native cells of the central nervous system. *Methods* **29:**326–334.

Fraticelli P, Sironi M, Bianchi G, D'Ambrosio D, Albanesi C, Stoppacciaro A, Chieppa M, Allavena P, Ruco L, Girolomoni G, et al. (2001) Fractalkine (CX3CL1) as an amplification circuit of polarized Th1 responses. *J Clin Investig* **107:**1173–1181.

Ghirnikar RS, Lee YL, and Eng LF (2000) Chemokine antagonist infusion attenuates cellular infiltration following spinal cord contusion injury in rat. *J Neurosci Res* **59:**63–73.

Ghirnikar RS, Lee YL, and Eng LF (2001) Chemokine antagonist infusion promotes axonal sparing after spinal cord contusion injury in rat. *J Neurosci Res* **64:**582–589.

Harrison JK, Fong AM, Swain PA, Chen S, Yu YR, Salafranca MN, Greenleaf WB, Imai T, and Patel DD (2001) Mutational analysis of the fractalkine chemokine domain. Basic amino acid residues differentially contribute to CX3CR1 binding, signaling and cell adhesion. *J Biol Chem* **276:**21632–21641.

Harrison JK, Jiang Y, Chen S, Xia Y, Maciejewski D, McNamara RK, Streit WJ, Salafranca MN, Adhikari S, Thompson DA, et al. (1998) Role for neuronally derived fractalkine in mediating interactions between neurons and CX3CR1-expressing microglia. *Proc Natl Acad Sci USA* **95:**10896–10901.

Haskell CA, Hancock WW, Salant DJ, Gao W, Csizmadia V, Peters W, Faia K, Fituri O, Rottman JB, and Charo IF (2001) Targeted deletion of CX(3)CR1 reveals a role for fractalkine in cardiac allograft rejection. *J Clin Investig* **108:**679–688.

Hoover DM, Mizoue LS, Handel TM, and Lubkowski J (2000) The crystal structure of the chemokine domain of fractalkine shows a novel quaternary arrangement. *J Biol Chem* **275:**23187–23193.

Imai T, Hieshima K, Haskell CA, Baba M, Nagira M, Nishimura M, Kakizaki M, Takagi S, Nomiyama H, Schall TJ, et al. (1997) Identification and molecular characterization of fractalkine receptor CX3CR1, which mediates both leukocyte migration and adhesion. *Cell* **91:**521–530.

Kansra V, Groves C, Gutierrez-Ramos JC, and Polakiewicz RD (2001) Phosphatidylinositol 3-kinase-dependent extracellular calcium influx is essential for CX(3)CR1-mediated activation of the mitogen-activated protein kinase cascade. *J Biol Chem* **276:**31831–31838.

Kledal TN, Rosenkilde MM, Coulin F, Simmons G, Johnsen AH, Alouani S, Power CA, Luttichau HR, Gerstoft J, Clapham PR, et al. (1997) A broad-spectrum chemokine antagonist encoded by Kaposi's sarcoma-associated herpesvirus. *Science (Wash DC)* **277:**1656–1659.

Kledal TN, Rosenkilde MM, and Schwartz TW (1998) Selective recognition of the membrane-bound CX3C chemokine, fractalkine, by the human cytomegalovirus-encoded broad-spectrum receptor US28. *FEBS Lett* **441:**209–214.

Lesnick P, Haskell CA, and Charo IF (2003) Decreased atherosclerosis in CX3CR1−/− mice reveals a role for fractalkine in atherogenesis. *J Clin Investig* **111:**333–340.

Liwang AC, Wang ZX, Sun Y, Peiper SC, and Liwang PJ (1999) The solution structure of the anti-HIV chemokine VMIP-II. *Protein Sci* **8:**2270–2280.

Luo Z, Fan X, Zhou N, Hiraoka M, Luo J, Kaji H, and Huang Z (2000) Structure-function study and anti-hiv activity of synthetic peptide analogues derived from viral chemokine VMIP-II. *Biochemistry* **39:**13545–13550.

Luttichau HR, Lewis IC, Gerstoft J, and Schwartz TW (2001) The herpesvirus 8-encoded chemokine VMIP-II, but not the poxvirus-encoded chemokine MC148, inhibits the CCR10 receptor. *Eur J Immunol* **31:**1217–1220.

Luttichau HR, Stine J, Boesen TP, Johnsen AH, Chantry D, Gerstoft J, and Schwartz TW (2000) A highly selective CC chemokine receptor (CCR)8 Antagonist encoded by the poxvirus molluscum contagiosum. *J Exp Med* **191:**171–180.

Matloubian M, David A, Engel S, Ryan JE, and Cyster JG (2000) A transmembrane CXC chemokine is a ligand for HIV-coreceptor Bonzo. *Nat Immunol* **1:**298–304.

McDermott DH, Fong AM, Yang Q, Sechler JM, Cupples LA, Merrell MN, Wilson PW, D'Agostino RB, O'Donnell CJ, Patel DD, et al. (2003) Chemokine receptor mutant CX3CR1–M280 has impaired adhesive function and correlates with protection from cardiovascular disease in humans. *J Clin Investig* **111:**1241–1250.

McDermott DH, Halcox JP, Schenke WH, Waclawiw MA, Merrell MN, Epstein N, Quyyumi AA, and Murphy PM (2001) Association between polymorphism in the chemokine receptor CX3CR1 and coronary vascular endothelial dysfunction and atherosclerosis. *Circ Res* **89:**401–407.

Meucci O, Fatatis A, Simen AA, and Miller RJ (2000) Expression of CX3CR1 chemokine receptors on neurons and their role in neuronal survival. *Proc Natl Acad Sci USA* **97:**8075–8080.

Mizoue LS, Bazan JF, Johnson EC, and Handel TM (1999) Solution structure and dynamics of the CX3C chemokine domain of fractalkine and its interaction with an N-terminal fragment of CX3CR1. *Biochemistry* **38:**1402–1414.

Mizoue LS, Sullivan SK, King DS, Kledal TN, Schwartz TW, Bacon KB, and Handel TM (2001) Molecular determinants of receptor binding and signaling by the CX3C chemokine fractalkine. *J Biol Chem* **276:**33906–33914.

Moatti D, Faure S, Fumeron F, Amara-Mel W, Seknadji P, McDermott DH, Debre P, Aumont MC, Murphy PM, de Prost D, et al. (2001) Polymorphism in the fractalkine receptor CX3CR1 as a genetic risk factor for coronary artery disease. *Blood* **97:**1925–1928.

Moore PS, Boshoff C, Weiss RA, and Chang Y (1996) Molecular mimicry of human cytokine and cytokine response pathway genes by KSHV. *Science (Wash DC)* **274:**1739–1744.

Murphy PM, Baggiolini M, Charo IF, Hebert CA, Horuk R, Matsushima K, Miller LH, Oppenheim JJ, and Power CA (2000) International Union of Pharmacology. XXII. Nomenclature for chemokine receptors. *Pharmacol Rev* **52:**145–176.

Nakano K, Isegawa Y, Zou P, Tadagaki K, Inagi R, and Yamanishi K (2003) Kaposi's sarcoma-associated herpesvirus (KSHV)-encoded VMIP-I and VMIP-II induce signal transduction and chemotaxis in monocytic cells. *Arch Virol* **148:**871–890.

Nicholas J, Ruvolo VR, Burns WH, Sandford G, Wan X, Ciufo D, Hendrickson SB, Guo HG, Hayward GS, and Reitz MS (1997) Kaposi's sarcoma-associated human herpesvirus-8 encodes homologues of macrophage inflammatory protein-1 and interleukin-6. *Nat Med* **3:**287–292.

Pan Y, Lloyd C, Zhou H, Dolich S, Deeds J, Gonzalo JA, Vath J, Gosselin M, Ma J, Dussault B, et al. (1997) Neurotactin, a membrane-anchored chemokine upregulated in brain inflammation. *Nature (Lond)* **387:**611–617.

Robinson LA, Nataraj C, Thomas DW, Howell DN, Griffiths R, Bautch V, Patel DD, Feng L, and Coffman TM (2000) A role for fractalkine and its receptor (CX3CR1) in cardiac allograft rejection. *J Immunol* **165:**6067–6072.

Rollins BJ (1997) Chemokines. *Blood* **90:**909–928.

Zhou N, Luo Z, Luo J, Hall JW, and Huang Z (2000) A novel peptide antagonist of CXCR4 derived from the N-terminus of viral chemokine VMIP-II. *Biochemistry* **39:**3782–3787.

Zujovic V and Harrison JK (2003) The chemokines and other cell migration regulating factors: fractalkine, in *The Cytokine Handbook*, 4th ed., vol II (Thomson AW and Lotze MT eds) pp 1101–1116, Academic Press, San Diego.

Address correspondence to: Dr. Jeffrey K. Harrison, Department of Pharmacology and Therapeutics, College of Medicine, University of Florida, P.O. Box 100267, Gainesville, FL 32610-0267. E-mail: harrison@pharmacology.ufl.edu